



## A multi-model study of the hemispheric transport and deposition of oxidised nitrogen

M. G. Sanderson,<sup>1</sup> F. J. Dentener,<sup>2</sup> A. M. Fiore,<sup>3</sup> C. Cuvelier,<sup>2</sup> T. J. Keating,<sup>4</sup> A. Zuber,<sup>5</sup> C. S. Atherton,<sup>6</sup> D. J. Bergmann,<sup>6</sup> T. Diehl,<sup>7</sup> R. M. Doherty,<sup>8</sup> B. N. Duncan,<sup>7</sup> P. Hess,<sup>9</sup> L. W. Horowitz,<sup>3</sup> D. J. Jacob,<sup>10</sup> J.-E. Jonson,<sup>11</sup> J. W. Kaminski,<sup>12</sup> A. Lupu,<sup>12</sup> I. A. MacKenzie,<sup>8</sup> E. Mancini,<sup>13</sup> E. Marmer,<sup>2</sup> R. Park,<sup>10,14</sup> G. Pitari,<sup>13</sup> M. J. Prather,<sup>15</sup> K. J. Pringle,<sup>1,16</sup> S. Schroeder,<sup>17</sup> M. G. Schultz,<sup>17</sup> D. T. Shindell,<sup>18</sup> S. Szopa,<sup>19</sup> O. Wild,<sup>20</sup> and P. Wind<sup>11</sup>

Received 18 July 2008; accepted 12 August 2008; published 13 September 2008.

[1] Fifteen chemistry-transport models are used to quantify, for the first time, the export of oxidised nitrogen ( $\text{NO}_y$ ) to and from four regions (Europe, North America, South Asia, and East Asia), and to estimate the uncertainty in the results. Between 12 and 24% of the  $\text{NO}_x$  emitted is exported from each region annually. The strongest impact of each source region on a foreign region is: Europe on East Asia, North America on Europe, South Asia on East Asia, and East Asia on North America. Europe exports the most  $\text{NO}_y$ , and East Asia the least. East Asia receives the most  $\text{NO}_y$  from the other regions. Between 8 and 15% of  $\text{NO}_x$  emitted in each region is transported over distances larger than 1000 km, with 3–10% ultimately deposited over the foreign regions.

**Citation:** Sanderson, M. G., et al. (2008), A multi-model study of the hemispheric transport and deposition of oxidised nitrogen, *Geophys. Res. Lett.*, 35, L17815, doi:10.1029/2008GL035389.

### 1. Introduction

[2] Oxidised nitrogen compounds, collectively referred to as  $\text{NO}_y$  (here,  $\text{NO}_y$  is the sum of the concentrations of  $\text{NO}$ ,  $\text{NO}_2$ ,  $\text{NO}_3$ ,  $\text{HNO}_3$ ,  $\text{HO}_2\text{NO}_2$ ,  $\text{NO}_3$ ,  $2 \times \text{N}_2\text{O}_5$ , organic nitrates and nitrate aerosols) play a central role in the chemistry of the atmosphere, particularly ozone formation [Seinfeld and Pandis, 2006]. Deposition of these compounds to water and soils is an important source of nutrients for many ecosystems. However, human activities, such as the burning of fossil fuels (which produce nitrogen oxides,  $\text{NO}_x$ , the sum of  $\text{NO}$  and  $\text{NO}_2$ ), have significantly perturbed the natural nitrogen cycle [Galloway et al., 2004]. The  $\text{NO}_x$

emitted undergoes rapid reaction to form the various  $\text{NO}_y$  species. Excessive deposition of nitrogen to ecosystems can cause eutrophication, where the extra nitrogen stimulates rapid plant growth and leads to a change in the species distribution and a loss of biodiversity. For example, Bergström and Jansson [2006] showed that inorganic nitrogen levels in lakes in Europe and North America have increased over the past 40 years, resulting in eutrophication and increased phytoplankton biomass. The results of the present work will be useful for other studies such as the International Nitrogen Initiative (<http://www.initrogen.org>), of whose aims one is to minimise the negative impact of nitrogen on the environment. The focus of the present work is on oxidised nitrogen species; deposition of reduced nitrogen species is also important, but is not considered here.

[3] There have been a few previous multi-model studies of nitrogen deposition. Holland et al. [1997] used five models to examine global nitrogen deposition and its impact on carbon uptake by vegetation. The latitudinal distributions and proportions of  $\text{NO}_y$  deposited to land varied considerably between the models. Lamarque et al. [2005] used results from six models to investigate changes in the deposition of  $\text{NO}_y$  between the years 2000 and 2100, using the IPCC SRES A2 scenario. They found significant increases in the future deposition fluxes, driven by greater emissions. The impact of climate change on regional deposition fluxes (a maximum of 50%) was greater than the modelled interannual variability (about 10%), but smaller than the impact of emissions increases (200–300%). Dentener et al. [2006] focused on global and

<sup>1</sup>Met Office Hadley Centre, Exeter, UK.

<sup>2</sup>European Commission, DG JRC, Institute for Environment and Sustainability, Ispra, Italy.

<sup>3</sup>NOAA Geophysical Fluid Dynamics Laboratory, Princeton, New Jersey, USA.

<sup>4</sup>Office of Policy Analysis and Review, Environmental Protection Agency, Washington, D. C., USA.

<sup>5</sup>Environment Directorate General, European Commission, Brussels, Belgium.

<sup>6</sup>Atmospheric Science Division, Lawrence Livermore National Laboratory, Livermore, California, USA.

<sup>7</sup>Goddard Earth Science and Technology Center, UMBC, Baltimore, Maryland, USA.

<sup>8</sup>School of GeoSciences, University of Edinburgh, Edinburgh, UK.

<sup>9</sup>National Center for Atmospheric Research, Boulder, Colorado, USA.

<sup>10</sup>Atmospheric Chemistry Modelling Group, Harvard University, Cambridge, Massachusetts, USA.

<sup>11</sup>Norwegian Meteorological Institute, Oslo, Norway.

<sup>12</sup>Center for Research in Earth and Space Science, York University, Toronto, Ontario, Canada.

<sup>13</sup>Dipartimento di Fisica, Università L'Aquila, Aquila, Italy.

<sup>14</sup>Now at School of Earth and Environmental Sciences, Seoul National University, Seoul, Korea.

<sup>15</sup>Earth System Science, University of California, Irvine, California, USA.

<sup>16</sup>Now at Max Planck Institute for Chemistry, Mainz, Germany.

<sup>17</sup>ICG-2, Forschungszentrum-Jülich, Jülich, Germany.

<sup>18</sup>NASA Goddard Institute for Space Studies and Columbia University, New York, New York, USA.

<sup>19</sup>Laboratoire des Science du Climat et de l'Environnement, Gif-sur-Yvette, France.

<sup>20</sup>Department of Environmental Science, Lancaster University, Lancaster, UK.

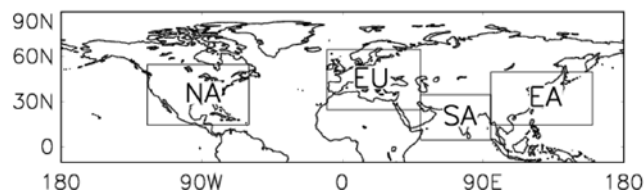


**Figure 1.** TF HTAP regions, EU (Europe), NA (North America), SA (South Asia) and EA (East Asia).

regional deposition fluxes of both oxidised and reduced nitrogen compounds for the present day and near future (2030), using an ensemble of 23 models. These authors calculated that 11% of the world's natural vegetation receives excess nitrogen through deposition, leading to eutrophication of ecosystems as discussed above. The emissions used in the study of *Dentener et al.* [2006] were prescribed, and so the spread in model deposition fluxes (between 30 and 50%) was mostly caused by differences in  $\text{NO}_y$  removal mechanisms between the models.

[4] However, it is not clear from these previous studies how much  $\text{NO}_y$  is exported from a given region, nor where regional emissions are ultimately deposited. The work described here is the first to use results from a series of multi-model experiments to quantify the impact of emissions of  $\text{NO}_x$  from each of four regions on the others, and estimate the associated uncertainty in the results. The four regions are Europe (EU), North America (NA), South Asia (SA) and East Asia (EA), and are illustrated in Figure 1. This work was carried out as part of a larger study of the intercontinental transport of both gaseous and aerosol species organised by the *Task Force on Hemispheric Transport of Air Pollution (TF HTAP)* [2007]. Since previous studies [e.g., *Schulz et al.*, 2006; *Stevenson et al.*, 2006; *Dentener et al.*, 2006] have shown that mean model results compare better with observations than any individual model, the focus in this paper is on the multi-model mean.

[5] The results have been used to calculate source-receptor relationships, defined as the response of the deposition of  $\text{NO}_y$  in a receptor region to a perturbation in the  $\text{NO}_x$  emission from a source region. Such source-receptor relationships provide useful information for policy makers [*Tarrasón et al.*, 2003]. These relationships imply that a change in emission in a given source region will result in a particular response at a receptor. The exact response in the receptor region will be dependent on the size of the perturbation in the source region. The areas of the four regions used here are large; use of emission perturbations in smaller areas may produce different source-receptor relationships. It should also be noted that the source-receptor relationships are calculated using a particular background state of the atmosphere, and that the relationships may be sensitive to changes in atmospheric composition.

[6] In this study, a 20% decrease in anthropogenic emissions was used, as it lies within the range of possible future regional emission reductions [*Cofala et al.*, 2007]. Previous results indicate that model responses to this size of emission change are close to linear [*TF HTAP*, 2007].

## 2. Models and Simulations

[7] Many different models have been used in the TF HTAP assessment of the hemispheric transport of pollutants; the

subset of 15 models used in the present work are described briefly in Table S1<sup>1</sup> (further details are at <http://www.htap.org>). Many of the models have been used in previous assessments of deposition fluxes [*Dentener et al.*, 2006]. Emissions of precursor gases ( $\text{NO}_x$ , CO, volatile organic compounds excluding methane, referred to as NMVOC and  $\text{SO}_2$ ) were not prescribed for this assessment; instead, each modelling group used their own best estimate of emissions for 2001. This course was followed because differences in emissions of both natural and anthropogenic precursor gases are an important source of uncertainty which we wished to include in our results (although the source-receptor relationships should be independent of the magnitude of the emissions). The global  $\text{NO}_x$  emissions and anthropogenic components in each HTAP region are listed in Table S2 for each model. The  $\text{NO}_x$  emissions show much less variation between models than those of CO or NMVOC. Global methane levels were fixed at 1760 ppb in all simulations, as this value is representative of the early 2000s [*Stevenson et al.*, 2006].

[8] All models used meteorology for 2001, and with two exceptions used either NCEP reanalyses, ECMWF analyses, NASA GEOS meteorological fields, or internally generated meteorology relaxed toward a reanalysis. Two models used monthly varying sea surface temperature and sea ice fields to drive their meteorology (Table S1). Each simulation was 1 year long, but all models were executed for a minimum of 6 months beforehand to bring the concentrations of reactive species into balance with the particular meteorology, emissions and chemical mechanisms used.

[9] The simulations consist of a control run, using the best estimate emissions for 2001, and a series of experiments where the anthropogenic emissions of  $\text{NO}_x$  were decreased by 20% in one of the four source regions (EU, NA, SA and EA; see Figure 1). For each experiment, the changes in  $\text{NO}_y$  deposition in each of these regions were examined. Previous work indicates that  $\text{NO}_y$  deposition fluxes are principally controlled by the location and magnitude of  $\text{NO}_x$  emissions [*Lamarque et al.*, 2005; *Sanderson et al.*, 2006]. To check this, results from a second series of experiments, in which anthropogenic emissions of all precursor gases ( $\text{SO}_2$ , CO, NMVOC and  $\text{NO}_x$ ) were reduced by 20% in each of the four source regions were also analysed. A comparison of these two series of experiments will illustrate the impact of any non-linearities in the chemistry of the different models. The ratio of the concentrations of  $\text{NO}_x$  to VOCs will clearly be different in the source region between the two sets of experiments, which in turn might impact on the proportions of the different  $\text{NO}_y$  species produced, and hence the amounts exported.

## 3. Results and Discussion

[10] A comparison of the multi-model mean wet deposition fluxes of  $\text{NO}_y$  with measured values are shown in Figure S1, using the same measurement data as *Dentener et al.* [2006]. Summary statistics for this comparison are presented in Table S3. Briefly, the mean model fluxes reproduce observed wet deposition fluxes well over NA and EU, but with more scatter for EA. The models under-

<sup>1</sup>Auxiliary materials are available in the HTML. doi:10.1029/2008GL035389.

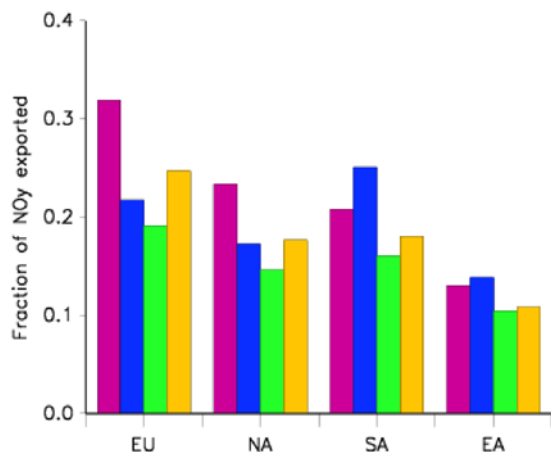


**Figure 2.** Export fractions of NO<sub>y</sub> from each HTAP region, for each season, Winter (pink), Spring (blue), Summer (green) and Autumn (yellow). The values shown are ensemble (15-model) means; see text for details.

estimate observed deposition fluxes over SA, by up to a factor of 4; it is likely that the emissions of NO<sub>x</sub> in this region used by the models are too low.

[11] We examine the change in the deposition flux of NO<sub>y</sub> in the receptor region divided by the size of the perturbation of NO<sub>x</sub> emissions in the source region, which we define to be the “sensitivity”. Although the absolute change in the deposition of NO<sub>y</sub> in a receptor region will depend on the size of the emission perturbation, the sensitivity will be independent of the emission perturbation, assuming a linear response from the models. The annual and seasonal mean sensitivities for each receptor region were calculated for each model; these individual results were then used to calculate the multi-model mean sensitivity and standard deviations.

[12] When the source and receptor regions are the same, subtracting the sensitivity from 1 gives the fraction of NO<sub>y</sub> that is exported; these export fractions are shown in Figure 2 for each season, using multi-model mean values. In the four regions shown in Figure 1, almost all of the NO<sub>x</sub> emissions result from anthropogenic activities, even with a 20% reduction. Many NO<sub>y</sub> species (e.g. HNO<sub>3</sub> and N<sub>2</sub>O<sub>5</sub>) are readily removed by dry and wet deposition, and so the lifetime of NO<sub>y</sub> is short. Hence, the majority of the NO<sub>x</sub> emitted is deposited within the continental-scale source regions. Between 12 and 24% of emitted NO<sub>x</sub> is exported out of the source regions as NO<sub>y</sub>. Of the four source regions, EA exports the least NO<sub>y</sub>, with little seasonality (between 0.10 and 0.15). The most NO<sub>y</sub> is exported from NA during winter and for SA during spring, although the difference between the seasons for each of these two regions is fairly small. EU exports more NO<sub>y</sub> than the other regions (0.24), and exports the most in winter (0.32). There is a greater spread of model results for winter than the other seasons.

[13] The annual mean sensitivities for each region to a 20% reduction in anthropogenic NO<sub>x</sub> emissions in each of the source regions are summarised in Table 1. The associated standard deviations (given in brackets after each value) give an indication of the spread in model results. The largest impacts of each region on another are EU on EA (2.4%), NA on EU (2.1%), SA on EA (6.4%) and EA on NA

(1.3%). These proportions should be compared with the amounts of NO<sub>y</sub> exported. For example, SA exports 20% of the NO<sub>x</sub> emitted, of which 32% is deposited in EA. The scatter in the model results is most likely to be due to differences in the boundary layer and convection schemes used to mix and transport the NO<sub>y</sub> species, and the associated wet removal processes. Overall, between 3 and 10% of NO<sub>x</sub> emitted in a HTAP region is deposited as NO<sub>y</sub> in the other three regions (assuming individual sensitivities combine linearly). Using the mean model results, between 51 and 66% of the exported NO<sub>y</sub> (or between 8 and 15% of NO<sub>x</sub> emitted) is transported over 1000 km from the boundaries of the source regions.

[14] The influence of the anthropogenic emissions of NO<sub>x</sub> from each of the four source regions on global NO<sub>y</sub> deposition is illustrated in Figure 3. Here, each panel shows the percentage reduction in the annual total NO<sub>y</sub> deposition fluxes in each of the NO<sub>x</sub> emission perturbation experiments, as compared with the control simulation, using multi-model mean values from each simulation. The emissions from NA and especially EU are clearly transported significant distances from the source regions and deposited over a wide area. EA emissions are transported across the Pacific to the west coast of NA, but no further. Conversely, the majority of the emissions from SA are deposited within the same region, or adjacent to it. In this latter case, a significant amount of the NO<sub>y</sub> will be removed by convective rainout; the high temperatures associated with SA promote thermal decomposition of insoluble PAN, and hence more wet deposition and less export of NO<sub>y</sub>.

[15] The sensitivities of the NO<sub>y</sub> deposition fluxes in the receptor regions when all anthropogenic emissions (CO, NMVOC, and SO<sub>2</sub>, as well as NO<sub>x</sub>) are reduced by 20% in each source region were also calculated (data not shown). A comparison with the previous results shows that the mean responses and uncertainties are generally similar, but not identical to those given in Table 1. For most source-receptor pairs the majority (10 or more) of the models gave a similar result, but there were instances where the sensitivities were different. This latter result suggests that there are some non-linear chemical effects on the formation and deposition of NO<sub>y</sub>, but the spread of results amongst the models is too large to allow a more definitive statement to be made.

[16] Deposition of NO<sub>y</sub> species occurs via both wet and dry processes, and the former is generally a more efficient removal process. The fraction of the NO<sub>y</sub> which is wet deposited may indicate one reason for the spread in the

**Table 1.** Source-Receptor Relationships for Each HTAP Region, When the Anthropogenic NO<sub>x</sub> Emissions are Reduced by 20% in the Source Region<sup>a</sup>

Source Region	Receptor Region			
	EU	NA	SA	EA
EU	76.2 (7.0)	0.7 (0.6)	2.2 (1.2)	2.4 (1.5)
NA	2.1 (0.8)	82.0 (5.4)	0.5 (0.3)	0.9 (0.5)
SA	1.3 (1.1)	0.8 (0.6)	80.6 (7.6)	6.4 (2.4)
EA	0.5 (0.3)	1.3 (0.8)	1.0 (0.4)	88.1 (5.7)

<sup>a</sup>Sensitivities are expressed as percentages; see text for definition. The values given here were calculated using annual mean results from 15 models. The standard deviations are given in brackets.

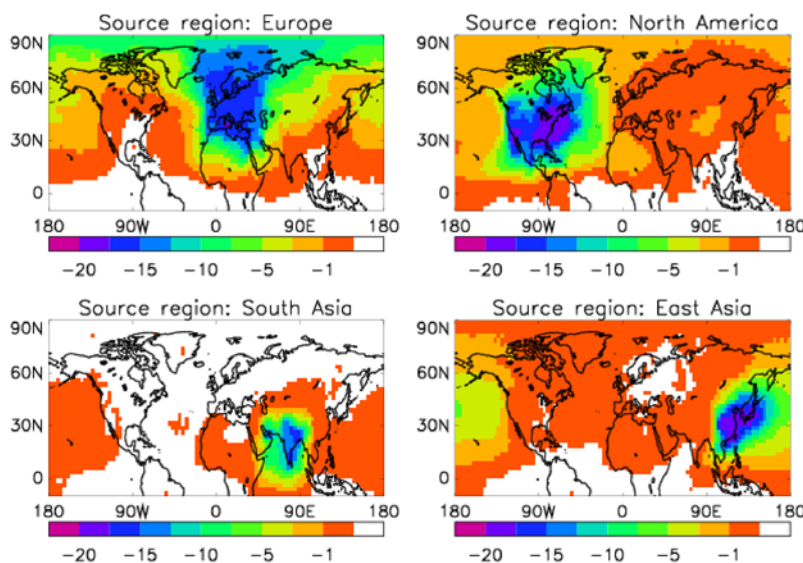


**Figure 3.** Percentage change in deposition of NO<sub>y</sub> in each NO<sub>x</sub> emission perturbation experiment relative to the control run, using multi-model annual mean deposition fluxes. The annual total deposition fluxes from each model were interpolated onto a 2.5° × 2.5° grid, from which the multi-model mean values were calculated; the data above are differences in the multi-model means. The white areas indicate a change in deposition of less than 0.1%.

model deposition fluxes, and hence in the fractions of NO<sub>y</sub> exported from a given region. For deposition to EU and NA, wet deposition accounts for about 0.3–0.6 of the total. For the two Asian regions (SA and EA), the wet deposition fraction lies between 0.4 and 0.7, similar to the estimates obtained by Lamarque *et al.* [2005]. The modelled deposition fluxes were found to be independent of the methane lifetime, suggesting that modelled OH abundances (which control the methane lifetime) do not control the NO<sub>y</sub> lifetimes. Another factor could be the efficiency of uptake of NO<sub>y</sub> by aerosols; an efficient uptake will reduce the NO<sub>y</sub> lifetime and hence the amounts available for long range transport.

#### 4. Conclusions

[17] Fifteen global chemistry-transport models have been used to assess the transport and deposition of NO<sub>y</sub> between four regions representing the major source areas. A source-receptor matrix was created using annual deposition totals. This matrix indicated that the largest impacts of Europe are on East Asia, North America on Europe, South Asia on East Asia, and East Asia on North America. 8–15% of NO<sub>x</sub> emitted from each region is transported over distances larger than 1000 km, and between 34 and 49% of the exported NO<sub>y</sub> is deposited within 1000 km. Between 3 and 10% of the NO<sub>x</sub> emitted from each region was deposited as NO<sub>y</sub> in the other three. These results, particularly the latter, suggest that the impact of intercontinental transport on regional NO<sub>y</sub> deposition is small. A continental scale focus on NO<sub>x</sub> emission controls might be the most effective policy to reduce nitrogen deposition fluxes.

[18] The differences between the deposition fluxes from the models will originate from many areas, including differing resolutions and the complexity of their chemical mechanisms. The fraction of NO<sub>y</sub> removed by wet deposi-

tion differs considerably between the models (see Table S2), and is likely to be a principal source of uncertainty in the source-receptor relationships; this process is more efficient at removing NO<sub>y</sub> than dry deposition. Some models do not include uptake of NO<sub>y</sub> by aerosols. Only one model simulates the formation, transport and deposition of ammonium nitrate. Some of the scatter in the sensitivities will be due to the different sources of meteorology, despite the same year being used. Some very recent work suggests that the formation of HNO<sub>3</sub> from the reaction between HO<sub>2</sub> and NO may have a significant impact on modelled NO<sub>y</sub> concentrations, and hence deposition fluxes [Cariolle *et al.*, 2008].

[19] The simulations used were only 1 year long, and so the influence of interannual variability on the derived source-receptor relationships via changes in the transport pathways cannot be assessed. Further experiments are currently underway, which use prescribed emissions and idealised species with fixed lifetimes and production rates to understand the impact of the different model transport processes on the results.

[20] **Acknowledgments.** This modelling exercise was organised under the Task Force for Hemispheric Transport of Air Pollution, which was set up by the Executive Body of the Convention on Long-Range Transboundary Air Pollution. MGS and KJP acknowledge funding from the UK Defra under contract AQ0409 and the Joint Defra and MoD Programme (Defra) GA01101 (MoD) CBC/2B/0417\_Annex C5. Work by CSA and DJB was performed under the auspices of the U.S. Department of Energy by Lawrence Livermore National Laboratory under Contract DE-AC52-07NA27.

#### References

- Bergström, A.-K., and M. Jansson (2006), Atmospheric nitrogen deposition has caused nitrogen enrichment and eutrophication of lakes in the Northern Hemisphere, *Global Change Biol.*, 12, 635–643, doi:10.1111/j.1365-2486.2006.01129.x.
- Cariolle, D., M. J. Evans, M. P. Chipperfield, N. Butkovskaya, A. Kukui, and G. Le Bras (2008), Impact of the new HNO<sub>3</sub>-forming channel of the

- HO<sub>2</sub> + NO reaction on tropospheric HNO<sub>3</sub>, NO<sub>x</sub>, HO<sub>x</sub> and ozone, *Atmos. Chem. Phys. Discuss.*, 8, 2695–2713.
- Cofala, J., M. Amann, Z. Klimont, K. Kupiainen, and L. Höglund-Isaksson (2007), Scenarios of global anthropogenic emissions of air pollutants and methane until 2030, *Atmos. Environ.*, 41, 8486–8499.
- Dentener, F. J., et al. (2006), Nitrogen and sulfur deposition on regional and global scales: A multimodel evaluation, *Global Biogeochem. Cycles*, 20, GB4003, doi:10.1029/2005GB002672.
- Galloway, J. N., et al. (2004), Nitrogen cycles: Past, present, and future, *Biogeochemistry*, 70, 153–226.
- Holland, E. A., et al. (1997), Variations in the predicted spatial distribution of atmospheric nitrogen deposition and their impact on carbon uptake by terrestrial ecosystems, *J. Geophys. Res.*, 102, 15,849–15,866.
- Lamarque, J.-F., et al. (2005), Assessing future nitrogen deposition and carbon cycle feedback using a multi-model approach: Analysis of nitrogen deposition, *J. Geophys. Res.*, 110, D19303, doi:10.1029/2005JD005825.
- Sanderson, M. G., W. J. Collins, C. E. Johnson, and R. G. Derwent (2006), Present and future acid deposition to ecosystems: The effect of climate change, *Atmos. Environ.*, 40, 1275–1283.
- Schulz, M., et al. (2006), Radiative forcing by aerosols as derived from the AeroCom present-day and pre-industrial simulations, *Atmos. Chem. Phys.*, 6, 5225–5246.
- Seinfeld, J. H., and S. N. Pandis (2006), *Atmospheric Chemistry and Physics: From Air Pollution to Climate Change*, 2nd ed., John Wiley, New York.
- Stevenson, D. S., et al. (2006), Multi-model ensemble simulations of present-day and near future tropospheric ozone, *J. Geophys. Res.*, 111, D08301, doi:10.1029/2005JD006338.
- Tarrasón, L., J. E. Jonson, H. Fagerli, A. Benedictow, P. Wind, D. Simpson, and H. Klein (2003), Transboundary acidification, eutrophication and ground level ozone in Europe Part III: Source-receptor relationships, *EMEP Status Rep. 2003*, Norw. Meteorol. Inst., Oslo, Norway.
- Task Force on Hemispheric Transport of Air Pollutants (TF HTAP) (2007), *Hemispheric Transport of Air Pollution 2007*, *Air Pollut. Stud.*, vol. 16, edited by T. J. Keating and A. Zuber, U. N. Econ. Comm. for Eur., Geneva, Switzerland. (Available at <http://www.htap.org>)
- C. S. Atherton and D. J. Bergmann, Atmospheric Science Division, Lawrence Livermore National Laboratory, Livermore, CA 94550, USA.
- C. Cuvelier, F. J. Dentener, and E. Marmer, European Commission, DG JRC, Institute for Environment and Sustainability, I-21020 Ispra, Italy.
- T. Diehl and B. N. Duncan, Goddard Earth Science and Technology Center, UMBC, Baltimore, MD 21228, USA.
- R. M. Doherty and I. A. MacKenzie, School of GeoSciences, University of Edinburgh, Edinburgh EH9 3JN, UK.
- P. Hess, National Center for Atmospheric Research, P.O. Box 3000, Boulder, CO 80307-3000, USA.
- A. M. Fiore and L. W. Horowitz, NOAA Geophysical Fluid Dynamics Laboratory, P.O. Box 308, Princeton, NJ 08542-0308, USA.
- D. J. Jacob, Atmospheric Chemistry Modelling Group, Harvard University, Cambridge, MA 02138, USA.
- J.-E. Jonson and P. Wind, Norwegian Meteorological Institute, P.O. Box 43 Blindern, N-0313 Oslo, Norway.
- J. W. Kaminski and A. Lupu, Center for Research in Earth and Space Science, York University, Toronto, ON M3J 1P3, Canada.
- T. J. Keating, Office of Policy Analysis and Review, Environmental Protection Agency, 1200 Pennsylvania Avenue, NW, Washington, DC 20760, USA.
- E. Mancini and G. Pitari, Dipartimento di Fisica, Università L'Aquila, I-67010 L'Aquila, Italy.
- R. Park, School of Earth and Environmental Sciences, Seoul National University, Seoul 151-747, Korea.
- M. J. Prather, Earth System Science, University of California, Irvine, CA 92697-3100, USA.
- K. J. Pringle, Max Planck Institute for Chemistry, P.O. Box 30 60, D-55020 Mainz, Germany.
- M. G. Sanderson, Met Office Hadley Centre, Exeter EX1 3PB, UK. ([michael.sanderson@metoffice.gov.uk](mailto:michael.sanderson@metoffice.gov.uk))
- S. Schroeder and M. G. Schultz, ICG-2, Forschungszentrum-Jülich, D-52425 Jülich, Germany.
- D. T. Shindell, NASA Goddard Institute for Space Studies, New York, NY 10025, USA.
- S. Szopa, Laboratoire des Science du Climat et de l'Environnement, F-Gif-sur-Yvette, France.
- O. Wild, Department of Environmental Science, Lancaster University, Lancaster LA1 4YQ, UK.
- A. Zuber, Environment Directorate General, European Commission, B-1049 Brussels, Belgium.